AN ANALYTIC TECHNIQUE FOR STATISTICALLY
MODELING RANDOM ATOMIC CLOCK ERRORS IN ESTIMATION

Patrick J. Fell

Naval Surface Weapons Center, Dahlgren, Virginia

ABSTRACT

Minimum variance estimation requires that the statistics of random observation errors be modeled properly. If measurements are derived through the use of atomic frequency standards, then one source of error affecting the observable is random fluctuation in frequency. This is the case, for example, with range and integrated Doppler measurements from satellites of the Global Positioning System used for precise geodetic point positioning and baseline determination for geodynamic applications. In this paper an analytic method is presented which approximates the statistics of this random process. The procedure starts with a model of the Allan variance for a particular oscillator and develops the statistics of range and integrated Doppler measurements. A series of five first order Markov processes is used to approximate the power spectral density obtained from the Allan variance. Range and Doppler error statistics are obtained from the integration of the corresponding autocorrelation function. Statistics for residuals to polynomial clock models are then obtained by linear transformation. Examples are given for rubidium and cesium clocks.

ATOMIC CLOCK ERRORS AND FREQUENCY STABILITY

A clock is any device which counts the cycles of a periodic phenomenon and among the most stable clocks in use are the atomic clocks which form the basis for atomic time scales such as International Atomic Time (TAI). Atomic time is used primarily as a measure of time interval and is based on the electromagnetic oscillations produced by quantum transitions within the atom. The precise definition of stability is found in Blair (1974). Basically it is a measure, usually given statistically, of the random fluctuations in frequency which can occur in a clock's oscillator over specified periods of time. For a given time interval a particular oscillator is considered best if the expected level of frequency fluctuation is a minimum in terms of the Allan variance defined below.

Equation (1) is the model used to describe the types of error present in atomic time scales

$$T_i(t) = \frac{1}{2} D_i(t - t_o)^2 + R_i(t - t_o) + T_i(t_o) + \tilde{x}(t) \tag{1}$$

The deterministic errors consist of bias, drift, and ageing terms modeled as a quadratic polynomial in time. The ageing term is less observable for clocks whose long-term stability is good such as cesium. The term $\tilde{x}(t)$ in equation (1) represents the random time error due to the integration of random fluctuations in frequency:

$$\tilde{x}(t) = \frac{1}{f_I} \int_{t_o}^{t} \tilde{f}(\tau)d\tau = \int_{t_o}^{t} y(\tau)d\tau . \tag{2}$$

The magnitude of this term depends on the stability of the clock and on the interval of time which has passed since the scale was reset or calibrated.

Hellwig (1977) points out that "the characterization of the stability of a frequency standard is usually the most important information to the user especially to those interested in scientific measurements and in the evaluation and intercomparison of the most advanced devices (clocks)." Since the frequency stability of a standard depends on a variety of physical and electronic influences both internal and external to the standard, measurement and characterization of frequency stability are always given subject to constraints on environmental and operating conditions. In addition frequency stability depends on the exact measurement procedure used to determine stability.

Frequency stability characterization is done in both the frequency and time domain. In the time domain a frequently used measure of stability is the Allan variance or its square root. In the frequency domain it is the power spectral density.

The Allan variance as a time domain measure of frequency stability is found especially useful in practice since it is obtainable directly from experimental measurements and contains all information on the second moments of the statistical distribution of fractional frequency error. The Allan variance is defined as follows: let y_0, y_1, y_2, · · ·., y_k, y_{k+1}, y_{k+2}, · · · be observed fractional frequency errors separated by a repetition interval of T seconds. For each integer N greater than or equal to 2, calculate $\bar{y}_m$ from

$$\bar{y}_m = \frac{1}{N} \sum_{k = mN}^{(m+1)N - 1} y_k \qquad m = 0, 1, 2, \ldots . M. \tag{3}$$

552

This is an average over N consecutive values of y_k. The Allan variance, $\sigma_y^2(N)$, is then obtained from the averages $\bar{y}_m$ by

$$\sigma_y^2(N) = \frac{1}{2M} \sum_{m=0}^{M-1} (\bar{y}_{m+1} - \bar{y}_m)^2. \tag{4}$$

An examination of this equation reveals that the Allan variance for a particular sampling interval NT is the average two-sample variance of the $\bar{y}_m(N)$.

For frequency standards the square root of the Allan variance is usually given in graphical form on a log-log scale. For individual classes of frequency standards models for the Allan variance are used which portray general frequency stability characteristics. Hellwig (1975) gives examples of such models for many oscillator types. Figure 1 shows the typical form. In this form, $\sigma_y(\tau)$ is the square root of the Allan variance for the sample interval τ. The quantity σ_f is called the flicker floor and τ_1, τ_2, τ_3 are the break points of the plot. The constants associated with this figure are usually specified for each type of frequency standard. A comparison of such information can facilitate the selection of a frequency standard for a specific application.

The stability characteristics shown in the three regions of Figure 1 are typically present in many Allan variance plots of specified oscillator performance. The first part, region I, reflects the fundamental noise properties of the standard. This behavior continues with increased sampling time until a floor is reached corresponding to region II. After τ_2 the performance deteriorates with increased sampling time. Hellwig (1977) outlines the error sources corresponding to each portion of the graph. The magnitude and slope of each segment will depend on the particular category of standard.

An alternative procedure for specifying the stability of a frequency standard, in the frequency domain, is the use of the power spectral density (PSD) of instantaneous fractional frequency fluctuations y(t). Allan et al. (1974) have given a useful model to represent the PSD for various categories of frequency standards. This model is in the form of a power law spectral density having the form

$$s_{yy}(\omega) = \begin{cases} h_\alpha \left(\dfrac{\omega}{2\pi}\right)^\alpha & 0 \le \omega \le \omega_h \\ 0 & \omega > \omega_h \end{cases} \tag{5}$$

where α takes on the integer powers between -2 and 2 inclusive depending on how the interval $(0, \omega_h)$ is to be divided into subintervals, one for each α to be used. The quantity h_α is a scaling constant, and the PSD is assumed to be negligible beyond the frequency range $(0, \omega_h)$.
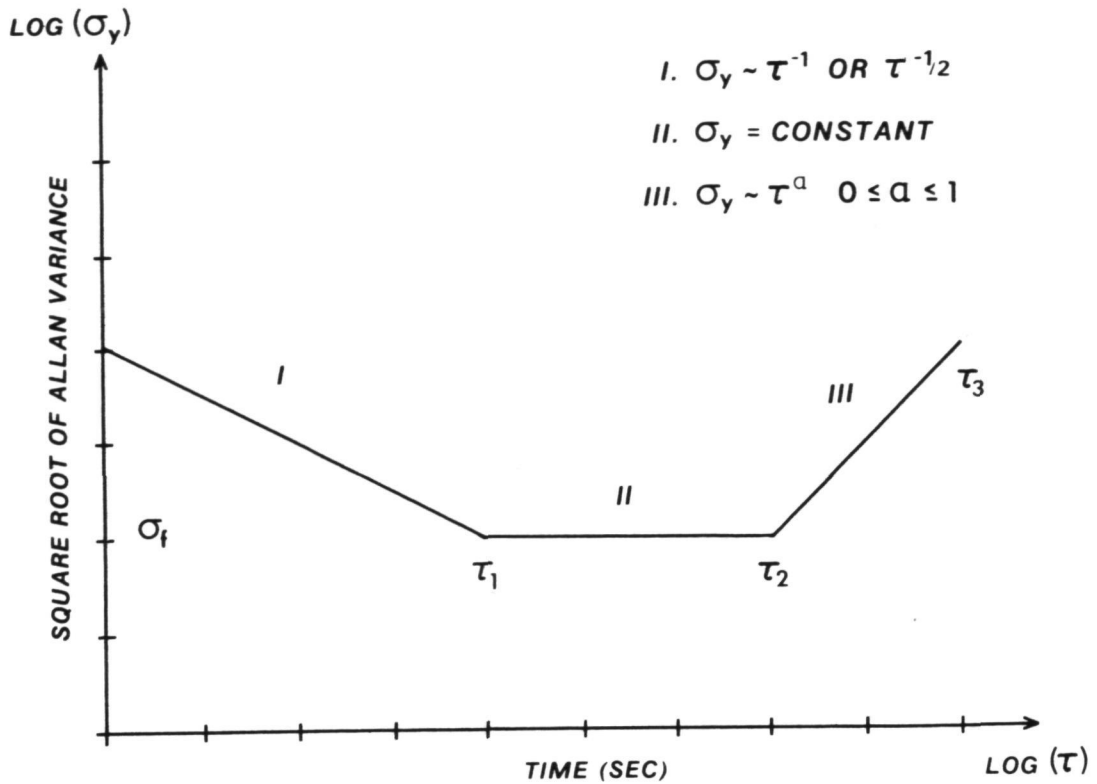
Fig. 1-General frequency stability characteristics

Barnes et al (1971) and Meditch (1975) give the transformations between the time domain measures of frequency stability in the form of the Allan variance and the power law spectral densities. Table 1 taken from Meditch gives these conversions for three types of fractional frequency error sources.

Table 1-Allan variance and power spectral
density for common error sources

ERROR SOURCE $y(t)$	ALLAN VARIANCE $\sigma^2_y(\tau)$	TWO SIDED SPECTRAL DENSITY $S_{yy}(\omega)$
WHITE NOISE	$\dfrac{N_0}{\tau}$	N_0
FLICKER NOISE	$\dfrac{2N_1 \ln 2}{\pi}$	$\dfrac{N_1}{|\omega|}$
INTEGRAL OF WHITE NOISE (RANDOM WALK)	$\dfrac{N_2 \tau}{3}$	$\dfrac{N_2}{\omega^2}$

554

RANGE AND DOPPLER OBSERVATION ERRORS DUE TO RANDOM ATOMIC CLOCK ERROR

As previously discussed, an atomic clock's time scale can be expected to differ from ideal time due to both deterministic and random errors. The random component is due to integration of fractional frequency errors. A range observation determined from radio signals broadcast by a satellite is subject to the random errors of the frequency standards in both the satellite and the tracking receivers. The effective range error at time t due to the timing error in one of the time scale is

$$\delta R_i(t) = cT_i(t) \tag{6}$$

with the random component being the random walk

$$\eta_i(t) = c \int_{t_s}^{t} y(\tau)d\tau \tag{7}$$

where c is the velocity of light. The random component is due to the accumulated effect of fractional frequency error since the clock's start or reset at t_s.

The random error $\eta_i(t)$ is correlated in time. Consider two measurements of range $R(t_j)$ and $R(t_k)$ based on the use of the oscillator in the satellite, and assume momentarily that the receiver's oscillator is free from random error. The covariance between these measured ranges due to correlated fractional frequency error in the satellite oscillator is

$$E[R(t_j)R(t_k)] = E[\eta(t_j)\eta(t_k)]$$

$$= c^2 E[\int_{t_s}^{t_j} y(\tau)d\tau \int_{t_s}^{t_k} y(\tau')d\tau']$$

$$= c^2 \int_{t_s}^{t_j} \int_{t_s}^{t_k} E[y(\tau)y(\tau')]d\tau d\tau'$$

$$= c^2 \int_{t_s}^{t_j} \int_{t_s}^{t_k} \phi_{yy}(\tau - \tau')d\tau d\tau' \tag{8}$$

where $\phi_{yy}(\tau - \tau')$ is the autocorrelation function for fractional frequency error y(t) defined by

$$\phi_{yy}(\tau - \tau') = E[y(\tau)y(\tau')]$$

$$= \int_{-\infty}^{\infty} \int_{-\infty}^{\infty} yy' f(y,y',\tau,\tau')dy\ dy'. \tag{9}$$

The function $f(y,y',\tau,\tau')$ is the joint probability density function for fractional frequency error. Here it is assumed that $y(t)$ is a mean zero stationary random process. The function $\phi_{yy}(\tau - \tau')$ could be obtained by the inverse Fourier transform of the given power spectral density $S_{yy}(\omega)$:

$$\phi_{yy}(t) = \frac{1}{2\pi} \int_{-\infty}^{\infty} S_{yy}(\omega)e^{i\omega t}d\omega \tag{10}$$

where

$$t = \tau - \tau'.$$

An alternate procedure for obtaining the autocorrelation function $\phi_{yy}(t)$ from the Allan variance is given below.

The variance of a range observation is obtained from equation (8) by setting t_j equal to t_k:

$$\sigma_{R_j}^2 = c^2 \int_{t_s}^{t_j} \int_{t_s}^{t_j} \phi_{yy}(\tau - \tau')d\tau d\tau'. \tag{11}$$

The presence of random frequency error in the receiver oscillator introduces additional, but similar, terms into equations (8) and (11) which must be considered when assessing the range uncertainty due to all random clock errors effecting the measurement.

For integrated Doppler or range difference observations the random measurement error associated with system clocks is the integral of fractional frequency error over the Doppler integration interval. The random error in range difference due to one oscillator is

$$\eta_{ij} = \eta(t_j) - \eta(t_k)$$

$$= c \int_{t_i}^{t_j} y(\tau)d\tau. \tag{12}$$

Notice in equation (12) that the random error η_{ij} is a function of t_i, t_j, and $y(t)$. The error does not depend on t_s. Range difference measurements have the following correlation for each oscillator

$$E[\Delta R_{ij} \Delta R_{k\ell}] = E[\eta_{ij} \eta_{k\ell}]$$

$$= c^2 \int_{t_i}^{t_j} \int_{t_k}^{t_\ell} \phi_{yy}(\tau - \tau')d\tau d\tau' \tag{13}$$

with the variance

$$\sigma_{\Delta R_{ij}}^2 = c^2 \int_{t_i}^{t_j} \int_{t_i}^{t_j} \phi_{yy}(\tau - \tau')d\tau d\tau'. \tag{14}$$

Observe that the random range difference errors, whose statistics are given by equations (13) and (14), are stationary; however, random range errors, whose statistics are given by equations (8) and (11), are not. A stationary random process is one whose statistics are invariant in time.

For the oscillator performance specifications shown in Figure 2 examples of the contribution to the range error are given for both oscillators in Figures 3 and 4 over a five-day span. The clocks are assumed to be perfect initially. Also included is the standard error for the random walk $\eta(t)$ obtained using equation (11). The procedure used in simulating the random range error is discussed in Meditch (1975).
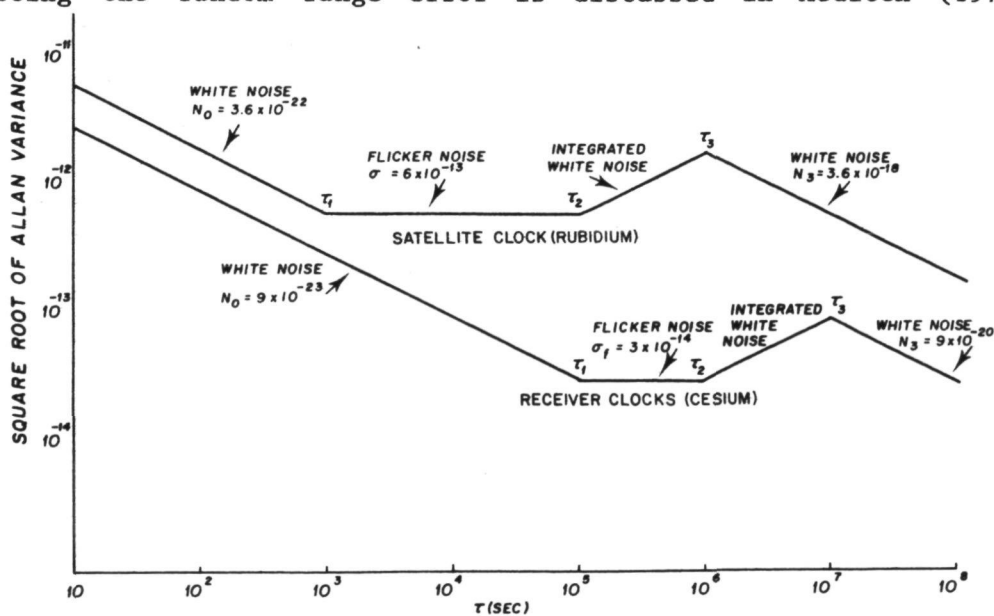

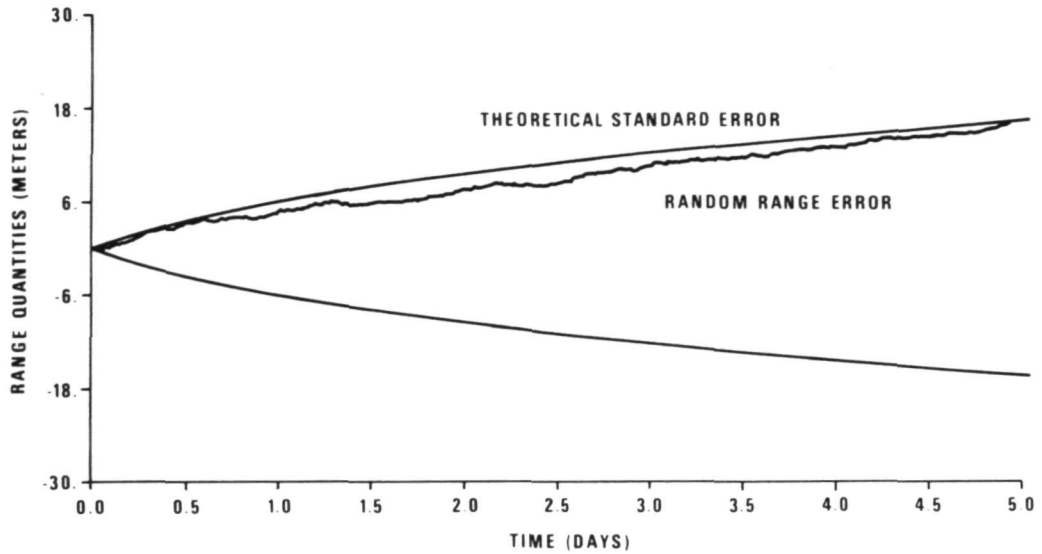Fig. 2-Allan variance for satellite and receiver oscillators

Fig. 3-Standard error and random range error
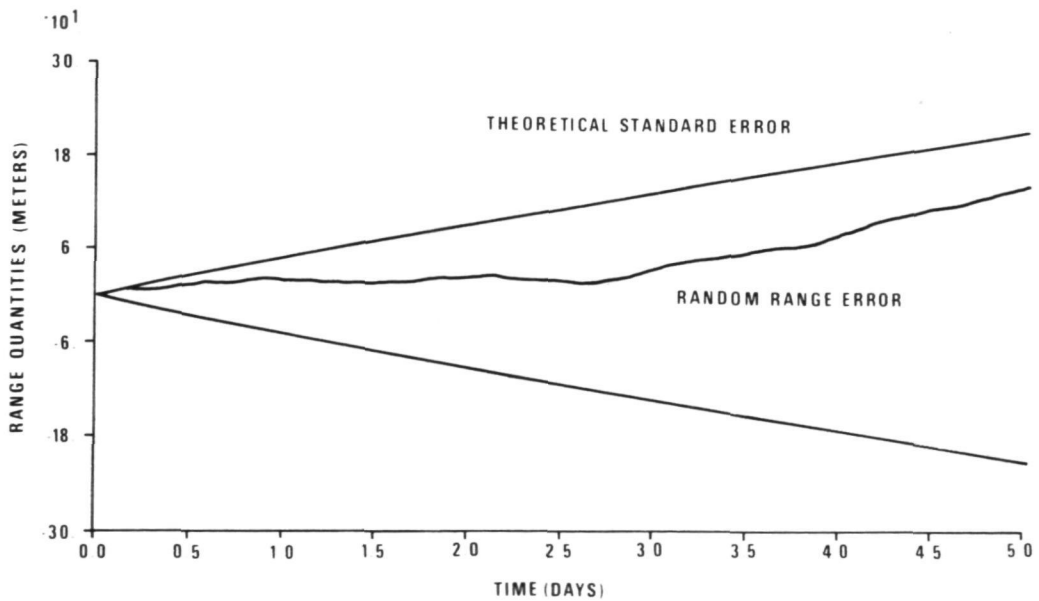based on receiver cesium specifications

Fig. 4-Standard error and random range error
based on satellite rubidium specifications

RANGE AND DOPPLER OBSERVATION ERROR STATISTICS

Fractional Frequency Autocorrelation from the Allan Variance

The equations giving the second order statistics of random range and
integrated Doppler observation errors due to random fractional fre-
quency errors were presented in the last section. Those equations
require that the fractional frequency autocorrelation function be
known. In this section discussion of a procedure for obtaining an
analytic approximation to this function from the Allan variance is
given. This method yields a simple analytic autocorrelation function
and avoids numerical difficulties that may arise when the inverse
Fourier transform of the power spectral density is evaluated.

The Allan variance models shown in Figure 2 for the satellite rubidium
and receiver cesium oscillators are a function of the sampling time τ
having the form

$$
\sigma_y^2(\tau) = \begin{cases}
\dfrac{N_0}{\tau} & \tau_\ell < \tau < \tau_1 \\[2ex]
\sigma_f^2 & \tau_1 < \tau < \tau_2 \\[2ex]
\dfrac{N_2 \tau}{3} & \tau_2 < \tau < \tau_3 \\[2ex]
\dfrac{N_3}{\tau} & \tau_3 < \tau < \infty.
\end{cases}
\tag{15}
$$

Using the transformations in Table 1 the power spectral density for
fractional frequency may be developed from equation (15):

$$
S_{yy}(\omega) = \begin{cases}
N_3 & 0 < \omega < \omega_0 \\[2ex]
\dfrac{N_2}{\omega^2} & \omega_0 < \omega < \omega_1 \\[2ex]
\dfrac{N_1}{\omega} & \omega_1 < \omega < \omega_2 \\[2ex]
N_0 & \omega_2 < \omega < \omega_h.
\end{cases}
\tag{16}
$$

The square roots of the power spectral densities corresponding to the
Allan variance specifications of Figure 2 are given in Figure 5. The
constants associated with the two functions and the formulas for
computing the constants associated with the power spectral density

559

function based on the Allan variance are given in Table 2. These formulas are developed from the transformations of Table 1.

The autocorrelation function $\phi_{yy}(t)$ can be obtained from the power spectral density using equation (10)

$$\phi_{yy}(t) = \frac{1}{2\pi} \int_{-\infty}^{\infty} S_{yy}(\omega) e^{i\omega t} d\omega.$$

However, as a result of transforming the band limited white noise portion of the spectrum, this form for the autocorrelation function has an oscillatory behavior for small t. This is an artificiality of the model.
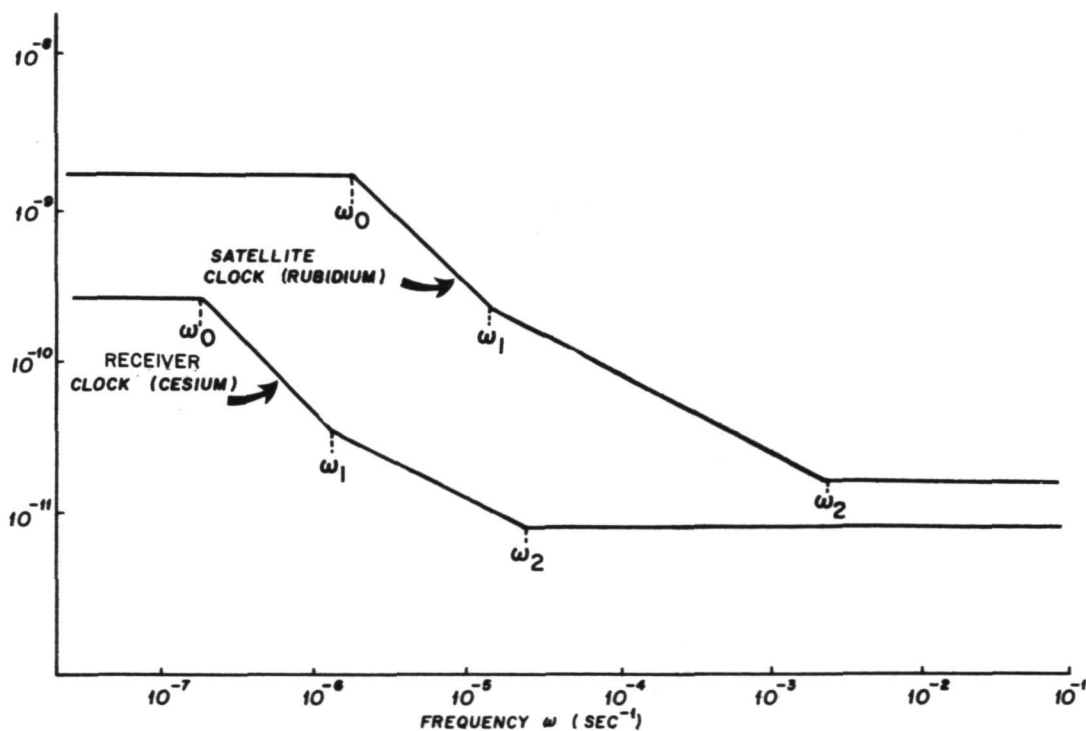

Fig. 5-Square root of PSD

An alternate approach for obtaining an autocorrelation function is to approximate the power spectral density model with a smooth function whose autocorrelation is expressible in simple analytic form. The first step in this development is to approximate the flicker noise

Table 2-Oscillator parameters

QUANTITY	UNITS	FORMULA	SATELLITE CLOCKS (RUBIDIUM)	RECEIVER CLOCK (CESIUM)
τ_1	sec		1.00×10^3	1.00×10^5
τ_2	sec		1.00×10^5	1.00×10^6
τ_3	sec		1.00×10^6	1.00×10^7
ω_0	sec^{-1}	$\sqrt{3}/\tau_3$	1.73×10^{-6}	1.73×10^{-7}
ω_1	sec^{-1}	$6 \ln 2/(\pi \tau_2)$	1.32×10^{-5}	1.32×10^{-6}
ω_2	sec^{-1}	$\pi/(2\tau_1 \ln 2)$	2.27×10^{-3}	2.27×10^{-5}
σ_f			6.00×10^{-13}	3.00×10^{-14}
N_0	sec	$\tau_1 \sigma_f^2$	3.60×10^{-22}	9.00×10^{-23}
N_1		$\pi \sigma_f^2/2 \ln 2$	8.16×10^{-25}	2.04×10^{-27}
N_2	sec^{-1}	$3\sigma_f^2/\tau_2$	1.08×10^{-29}	2.70×10^{-33}
N_3	sec	$\sigma_f^2 \tau_3^2/\tau_2$	3.60×10^{-18}	9.00×10^{-20}
α		$(\omega_2/\omega_1)^{1/6}$	2.36×10^0	1.61×10^0
ω_a	sec^{-1}	$\omega_1\sqrt{\alpha}$	2.03×10^{-5}	1.67×10^{-6}

segment of the spectrum by a series of cascading functions whose values alternate between being constant and being inversely proportional to the square of the frequency. This type of procedure is described by Meditch (1975) in constructing a linear system which simulates flicker noise using a white noise input. Figure 6 shows the transfer function for flicker noise. A three stage cascading transfer function is superimposed consisting of the functions F_A, F_B, and F_C which are defined in Table 3. These functions are defined to have the required properties and give a continuous although not smooth approximation to the flicker noise power spectral density.

The constants of this approximation are now derived over frequency intervals as given in Meditch (1975). The general form of the function F_A is

$$F_A(\omega) = \frac{N_A}{\omega_a^2} \tag{17}$$

between the frequencies ω_a and $\alpha\omega_a$. At frequency ω_a, defined in Table 2, the function F_A takes on the value
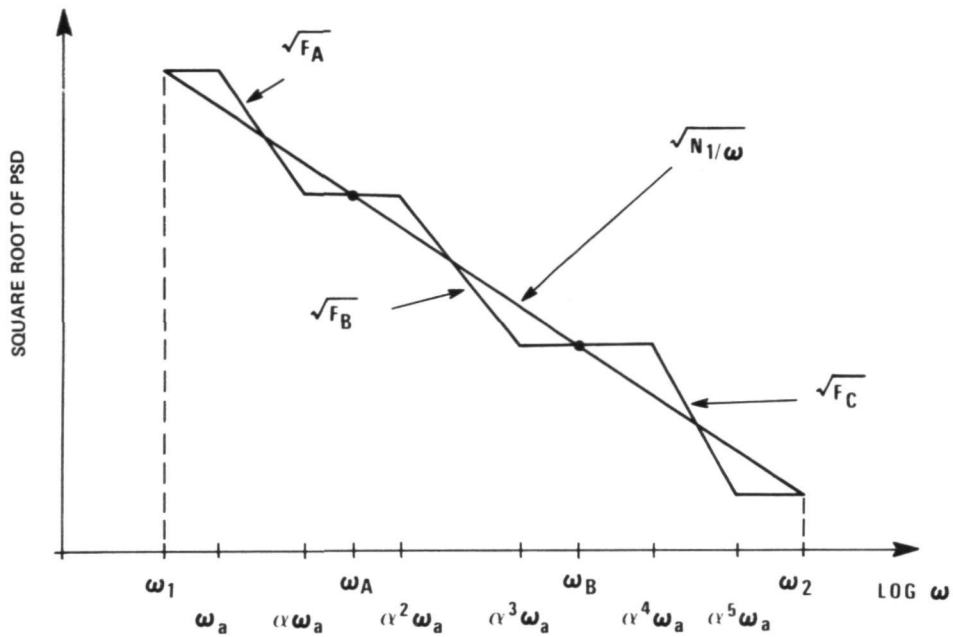
561

Fig. 6-Three stage transfer function approximation
of flicker noise spectrum

Table 3-Definition of three stage transfer function approximation

FUNCTION	INTERVAL	DEFINITION (PSD)
	$\omega_1 \leqslant \omega \leqslant \omega_a$	N_1/ω_1
F_A	$\omega_a \leqslant \omega \leqslant a\omega_a$	N_A/ω^2
	$a\omega_a \leqslant \omega \leqslant \omega_A$	$N_A/a^2\omega_a{}^2$
	$\omega_A \leqslant \omega \leqslant a^2\omega_a$	$N_A/a^2\omega_a{}^2$
F_B	$a^2\omega_a \leqslant \omega \leqslant a^3\omega_a$	N_B/ω^2
	$a^3\omega_a \leqslant \omega \leqslant \omega_B$	$N_B/a^6\omega_a{}^2$
	$\omega_B \leqslant \omega \leqslant a^4\omega_a$	$N_B/a^6\omega_a{}^2$
F_C	$a^4\omega \leqslant \omega \leqslant a^5\omega_a$	N_C/ω^2
	$a^5\omega \leqslant \omega \leqslant \omega_2$	N_o

WHERE

$$N_A = a\omega_1 N_1$$

$$N_B = a^3\omega_1 N_1$$

$$N_C = a^5\omega_1 N_1$$

$$a = \left(\frac{\omega_2}{\omega_1}\right)^{\frac{1}{2n}}$$

$$\omega_a = \omega_1\sqrt{a}$$

$$n = 3$$

$$F_A(\omega_a) = \frac{N_A}{\omega_a^2} = \frac{N_1}{\omega_1} \tag{18}$$

since the flicker noise power spectral density has the same function value at frequency ω_1. Solving equation (18) gives

$$N_A = \frac{N_1\omega_a^2}{\omega_1} = \alpha\omega_1 N_1. \tag{19}$$

A similar analysis gives the constant N_B. The function F_B has the form

$$F_B(\omega) = \frac{N_B}{\omega^2}. \tag{20}$$

At frequency $\alpha^2\omega_a$, F_B has the function value

$$F_B(\alpha^2\omega_a) = \frac{N_B}{\alpha^4\omega_a^2} = \frac{N_A}{\alpha^2\omega_a^2} \tag{21}$$

since at $\alpha^2\omega_a$ the function F_B has the same value as function F_A at frequency $\alpha\omega_a$ (see Figure 6). Solving equation (21) and using equation (19)

$$N_B = \alpha^2 N_A = \alpha^3\omega_1 N_1. \tag{22}$$

For the function F_C,

$$F_C(\omega) = \frac{N_C}{\omega^2} \tag{23}$$

its function value at frequency $\alpha^4\omega_a$ equals the value of F_B at frequency $\alpha^3\omega_a$ giving

$$F_C(\alpha^4\omega_a) = \frac{N_C}{\alpha^8\omega_a^2} = \frac{N_B}{\alpha^6\omega_a^2} . \tag{24}$$

Using equation (22) gives the solution

$$N_C = \alpha^2 N_B = \alpha^5\omega_1 N_1. \tag{25}$$

Numerical values for α and ω_a are given in Table 2. The power spectral density consisting of the three cascading functions and the remainder of the original function will be denoted as the second power spectral density model for each oscillator.

The next step in the development of a simple analytic autocorrelation function is to approximate various segments of this second model with a first order Markov process power spectral density function, a function of the form

$$S(\omega) = \frac{2\sigma^2\beta}{\omega^2 + \beta^2} \tag{26}$$

where β is the inverse of the correlation time (see Gelb (1974)). The autocorrelation function for a first order Markov process is

$$\Phi(t) = \sigma^2 e^{-\beta t} . \tag{27}$$

Notice in equation (26) that the power spectral density decreases as the inverse of the square of the frequency. This is the type of functional behavior seen in the interior of the cascading functions F_A through F_C. It is also the behavior of the original power spectral density in the interval (ω_0, ω_1). In addition the power spectral density of the Markov process remains virtually flat until the frequency reaches a point at which the function decreases rapidly. These properties make this function an excellent choice for approximating the second power spectral density model piecewise.

The second model is then divided into five segments defined in Table 4. The high frequency cut off ω_h, shown as 10^{-1} in Figure 5, will be increased so that the band limited white noise component of the power spectral density may be approximated better by the first order Markov power spectral density.

Table 4-Division of second PSD model for Markov process approximation

NOTATION	INTERVAL
I_1	$[0, \omega_1]$
I_2	$[\omega_1, \alpha\omega_a]$
I_3	$[\alpha\omega_a, \alpha^3\omega_a]$
I_4	$[\alpha^3\omega_a, \alpha^5\omega_a]$
I_5	$[\alpha^5\omega_a, \omega_h]$

The approximation consists then of fitting a function in the form of equation (26) to each subdivision of the second model $S'_{yy}(\omega)$ given in Table 4. There are two parameters σ and β to be determined for each segment giving a total of ten parameters.

The procedure which was adopted was an asymptotic approximation whereby two constraints were imposed on the Markov power spectral density function giving σ and β directly. This procedure was implemented because of simplicity and because the results compared favorably with a least squares approach. The asymptotic approach develops an approximation on the interval I_j,

$$I_j \sim [\omega_k, \omega_\ell]$$

using the following constraints:

(i) at zero frequency the approximating Markov power spectral density equals the second model at frequency ω_k:

$$S_j(o) = S'_{yy}(\omega_k) \tag{28}$$

(ii) in the limit as ω increases the value of the function $S_j(\omega)$ converges to the following function

$$\lim_{\omega \to \infty} S_j(\omega) = \frac{2\sigma^2\beta}{\omega^2} \tag{29}$$

and at ω_ℓ this limiting value is set equal to the value of $S'_{yy}(\omega)$:

$$\frac{2\sigma^2\beta}{\omega_\ell^2} = S'_{yy}(\omega_\ell). \tag{30}$$

Equations (28) and (30) are a system of two equations in two unknowns. Their solution yields the parameters σ_j and β_j for the approximating Markov power spectral density function $S_j(\omega)$. The nature of the second constraint, equation (30), is to force the function $S_j(\omega)$ to asymptotically approach $S'_{yy}(\omega)$ at ω_ℓ. The first constraint is necessary to approximate the white noise or flat component of $S'_{yy}(\omega)$ at the beginning of each subinterval.

Finally a comment concerning the approximation in the last subdivision I_5 is necessary. In order to obtain a good approximation to $S'_{yy}(\omega)$ in that interval it is necessary to choose ω_h large enough to allow the

flat portion of the Markov process spectral density to fit the white noise component which dominates this interval (see Figure 5). Choosing w_h three or four orders of magnitude larger than 0.1 and $S_{yy}'(w_h)$ two or three orders of magnitude smaller than N_0, enables a good approximation to be made but adds power at these higher frequencies. The result is an autocorrelation function which tends to a delta function as w_h goes to infinity and whose variance increases as w_h is chosen larger (see Figure 7). However, this will have negligible effect on range and range difference statistics.

The smooth fractional frequency autocorrelation function $\phi_{yy}(t)$ is given by the inverse Fourier transform of the five Markov process power spectral densities $S_j(w)$. The result of each transformation is an analytic function whose form is given by equation (27). The final result is the sum of these functions

$$\phi_{yy}(t) = \sum_{j=1}^{5} \sigma_j^2 e^{-\beta_j |t|} . \tag{31}$$

For range and integrated Doppler observations the statistical contribution due to random oscillator error is obtained using equation (31) in equation (8) through (14).

Figures 8 and 9 show the original transfer functions and the asymptotic approximations. The parameters obtained using this approximation procedure are given in Table 5.

Observation Error Statistics Based on Markov Process Approximations

The first order Markov autocorrelation function, equation (31), and equations (8) through (14) give the second order statistics for random range and integrated Doppler observation errors due to each oscillator used in the measurement process. These integrals may be evaluated giving analytical expressions for the variance and covariance of range and Doppler observations.

Let $R(t_i)$ and $R(t_k)$ be range observations subject to one random clock error only. The covariance between the observations is given by equation (8). Using the first order Markov approximations, the integration of equation (8) gives the covariance as
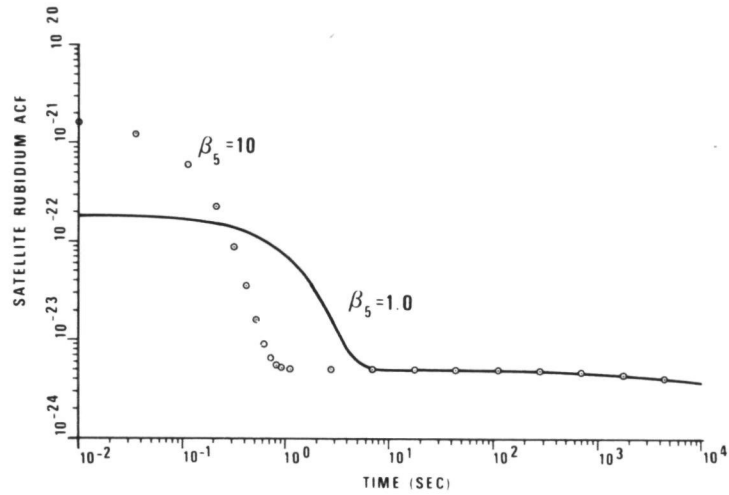
Fig. 7-Asymptotic fractional frequency autocorrelation
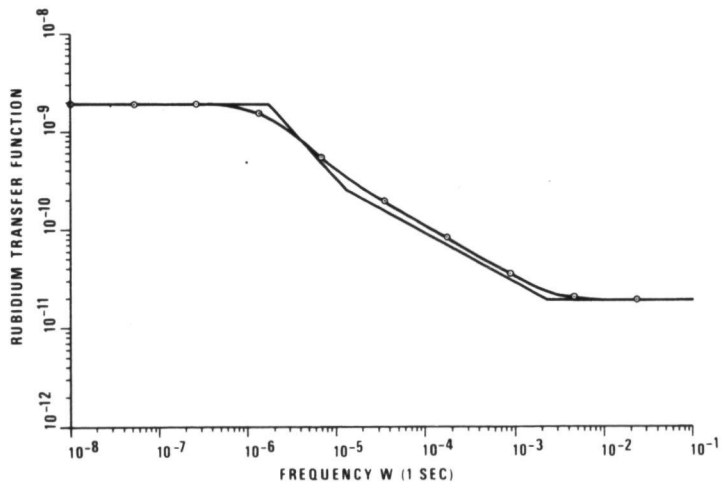functions based on Markov process approximations

Fig. 8-Satellite oscillator transfer function and sum
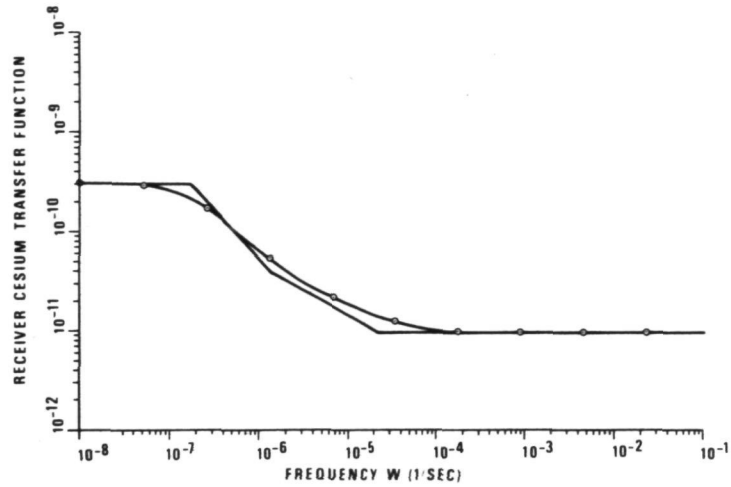of asymptotic approximations

Fig. 9-Receiver cesium transfer function and sum
of asymptotic approximations

Table 5-Fractional frequency autocorrelation function
parameters for Markov process approximations

OSCILLATOR TYPE	INTERVAL	ASSYMPTOTIC		LEAST SQUARES	
		$(ALPHA)^2$	BETA	$(ALPHA)^2$	BETA
RUBIDIUM (SPEC)	I_1	3.1177×10^{-24}	1.732×10^{-6}	3.3719×10^{-24}	1.681×10^{-6}
	I_2	6.2625×10^{-25}	2.032×10^{-5}	7.6238×10^{-25}	2.255×10^{-5}
	I_3	6.2625×10^{-25}	1.128×10^{-4}	7.6245×10^{-25}	1.252×10^{-4}
	I_4	6.2625×10^{-25}	6.262×10^{-4}	7.6245×10^{-25}	6.947×10^{-4}
	I_5	1.8000×10^{-19}	$1.000 \times 10^{3*}$	1.9343×10^{-19}	$9.631 \times 10^{2*}$
CESIUM (SPEC)	I_1	7.7942×10^{-27}	1.732×10^{-7}		
	I_2	1.2922×10^{-27}	1.677×10^{-6}		
	I_3	1.2922×10^{-27}	4.321×10^{-5}		
	I_4	1.2922×10^{-27}	1.113×10^{-5}		
	I_5	4.5000×10^{-20}	$1.000 \times 10^{3*}$		

$^*\omega_h = 1.0 \times 10^4$ $S'\gamma\gamma(\omega_h) = N_0/1.0 \times 10^2$

568

$$E[R(t_i)R(t_k)] = E[\eta(t_i)\eta(t_k)]$$

$$= c^2 \sum_{j=1}^{5} \frac{\sigma_j^2}{\beta_j} \left[2(t_i - t_s) + \frac{1}{\beta_j} \left(e^{-\beta_j(t_j - t_s)} \right. \right.$$

$$\left. \left. + e^{-\beta_j(t_k - t_s)} - e^{-\beta_j(t_k - t_i)} - 1 \right) \right] \tag{32}$$

for t_k greater than t_i, where t_s is the start or reset time of the clock. The variance of the random range error is obtained by setting t_k equal to t_i in equation (32)

$$E[R(t_i)R(t_i)] = E[\eta(t_i)\eta(t_i)]$$

$$= c^2 \sum_{j=1}^{5} \frac{2\sigma_j^2}{\beta_j} \left[(t_i - t_s) \right.$$

$$\left. + \frac{1}{\beta_j} \left(e^{-\beta_j(t_i - t_s)} - 1 \right) \right]. \tag{33}$$

The range error $\eta(t)$ resulting from the integration of fractional frequency error $y(t)$ is a statistically nonstationary process. An examination of equations (32) and (33) reveals terms which are functions of t_i, or t_k, minus t_s. Thus, for instance, the variance increases with time. This is illustrated in Figure 10 for the rubidium clock. The standard error of a range measurement based on the use of this clock is given for 20 range observations spaced at 15-minute intervals starting five minutes, one hour, and five hours after the start of the clock. The increase in variance is almost linear. An examination of the autocorrelation function shows that this function, dominately flat, is similar to a random bias having a constant autocorrelation and whose integral is a random ramp which increases exactly linearly. Hence a linear growth in variance is expected as seen in Figure 10. The correlation coefficients ρ_{1i} between the first and the i'th range observation in each of these sequences are given in Figure 11. As the starting time of the sequence increases from t_s, so does the correlation among the random errors. This again is expected, since the variance increases with time and the errors are correlated.

Figure 12 gives the autocorrelation function for the cesium clock based on the Markov process approximation and Figures 13 and 14 give the standard error and correlations of range errors based on this clock. A comparison of Figures 10 and 13 reveals the greater stability of the cesium clock. After ten hours of operation the standard error of the cesium clock output is approximately 3.5 nanoseconds compared to 63
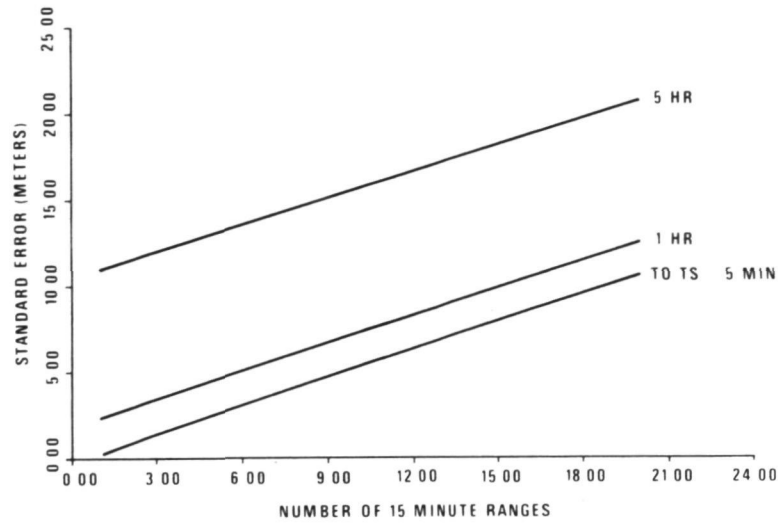
Fig. 10-Standard error of range observations
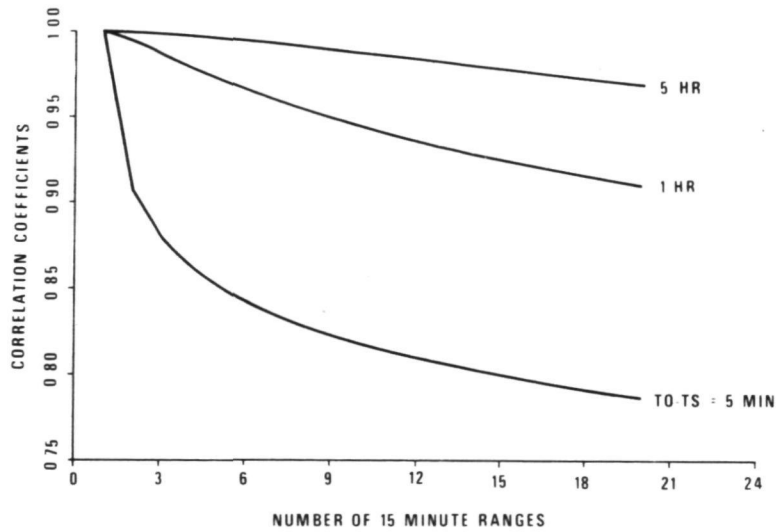based on satellite rubidium oscillator

Fig. 11-Correlation coefficients between range 1
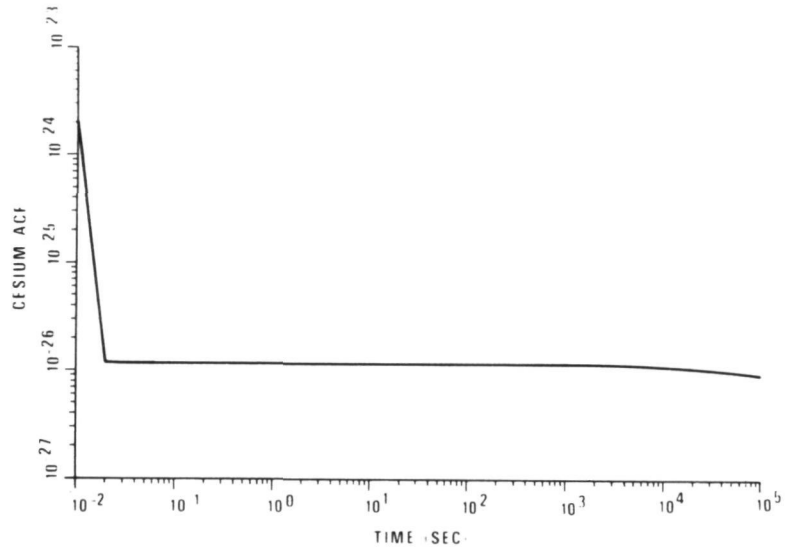and range i (rubidium clock)

Fig. 12-Asymptotic fractional frequency autocorrelation
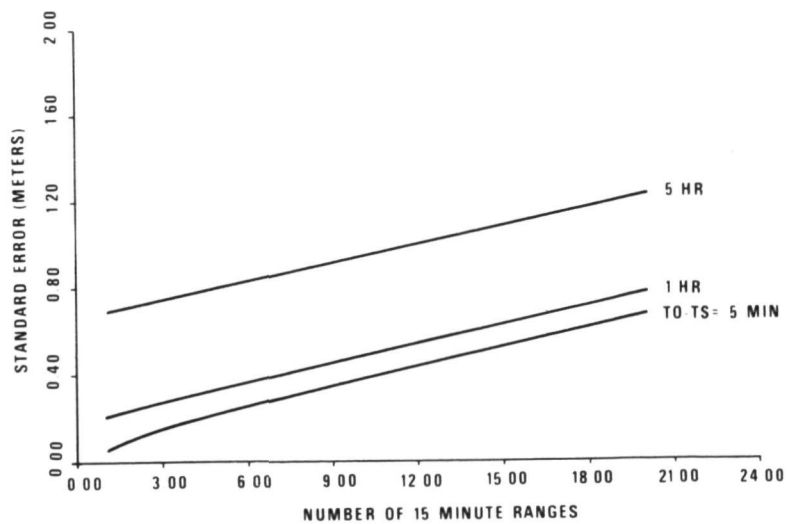function for cesium standard

Fig. 13-Standard error of range observations
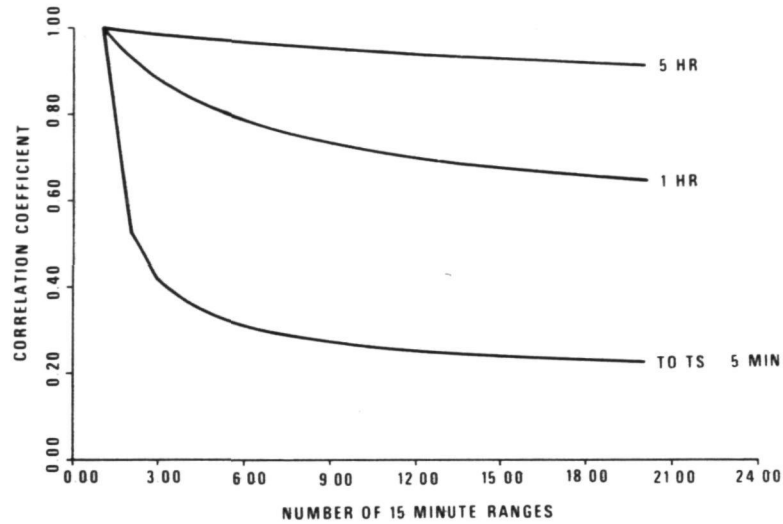based on cesium oscillator

571

Fig. 14-Correlation coefficients between
range 1 and range i (cesium clock)

nanoseconds for the rubidium standard. In addition, the correlations among the cesium clock errors decrease more rapidly than the rubidium clock errors. Considering both random clock error sources the total variance and correlation of range observations $R_k(t_i)$ and $R_k(t_j)$ measured by receiver k are given by the equations

$$E[R_k(t_i)R_k(t_i)] = E[\eta_s(t_i)\eta_s(t_i)] + E[\eta_k(t_i)\eta_k(t_i)] \qquad (34)$$

$$E[R_k(t_i)R_k(t_j)] = E[\eta_s(t_i)\eta_s(t_j)] + E[\eta_k(t_i)\eta_k(t_j)] \qquad (35)$$

where the variances and correlations of the random error η are given by equations (32) and (33). The subscript "s" refers to the satellite rubidium clock.

For simultaneous observations of range by two receivers the covariance of the observations $R_k(t_i)$ and $R_\ell(t_j)$ is given by

$$E[R_k(t_i)R_\ell(t_j)] = E[\eta_s(t_i)\eta_s(t_j)]. \qquad (36)$$

In the above equations the random errors η have zero mean which is a consequence of fractional frequency error being zero mean.

Let $\Delta R(t_n)$ be an integrated Doppler or range difference measurement over the interval $(t_i,\ t_n)$ and $\Delta R(t_\ell)$ a similar measurement from the

572

same receiver over the interval (t_k, t_ℓ). The covariance of the observations is

$$
\begin{aligned}
E[\Delta R(t_n), \Delta R(t_\ell)] &= E[\eta(t_n) - \eta(t_i), \eta(t_\ell) - \eta(t_k)] \\
&= E[\eta(t_n)\eta(t_\ell)] - E[\eta(t_n)\eta(t_k)] - E[\eta(t_i)\eta(t_w)] \\
&\quad + E[\eta(t_i)\eta(t_k)] \\
&= c^2 \sum_{j=1}^{5} \frac{\sigma_j^2}{\beta_j^2} \left[e^{-\beta_j(t_\ell - t_n)} - e^{-\beta_j(t_k - t_n)} \right. \\
&\quad \left. - e^{-\beta_j(t_\ell - t_i)} + e^{-\beta_j(t_k - t_i)} \right].
\end{aligned}
\tag{37}
$$

The variance of a range difference observation is given by

$$
E[\Delta R(t_n)\Delta R(t_n)] = c^2 \sum_{j=1}^{5} \frac{2\sigma_j^2}{\beta_j} \left[(t_n - t_i) + \frac{1}{\beta_j}\left(e^{-\beta_j(t_n - t_i)} - 1\right) \right].
\tag{38}
$$

Equations (37) and (38) are independent of the clock epoch t_s. The statistics of the range difference error depend only on the Doppler integration interval or the time difference between observations. Thus the random range difference error is stationary. Expressions analogous to equations (34) through (36) express the complete statistics of range difference observation errors for individual or simultaneous observations due to clock error.

STATISTICS OF RESIDUALS TO POLYNOMIAL CLOCK MODELS

The statistical characteristics of fractional frequency error and its integrated effect on range and Doppler observations have been discussed in detail. For range observations assume that the total random error is due to three sources, two of which are correlated noise processes. Then the total random range error is expressed as

$$
\eta(t) = \eta_s(t) + \eta_k(t) + \xi(t)
\tag{39}
$$

where η_s and η_k are the correlated random range errors due to satellite and receiver random clock errors respectively. The quantity ξ represents receiver white noise. The total integrated Doppler random error over the integration interval $[t_j, t_\ell]$ is

$$
\Delta\eta(t_\ell) = \eta_s(t_\ell) - \eta_s(t_j) + \eta_k(t_\ell) - \eta_k(t_j) + \zeta_\ell
\tag{40}
$$

573

where ζ_ℓ is the white noise associated with the Doppler measurement procedure.

Depending on the stability of the clock, the random range or Doppler error components, $\eta_s(t)$ and $\eta_k(t)$, may appear quite systematic over fixed time intervals and may be represented by polynomial models of varying degree. For short time intervals the models for clock error were taken to be a bias and drift for range observations and a frequency bias for Doppler observations. However, these models and even higher order polynomial models are not sufficient to entirely represent this correlated error. Thus knowledge of the statistical properties of the deviations of the error from such a model becomes important, as these residuals represent an unmodeled part of the observation equation after the inclusion of the polynomial model.

Proceeding, equation (39) is expressed as follows

$$\eta(t) = P_{ms}(t) + P_{nk}(t) + r_s(t) + r_k(t) + \xi(t) \tag{41}$$

where $P_{ms}(t)$ is an m'th degree polynomial chosen to model the correlated random error $\eta_s(t)$ and $P_{nk}(t)$ is an n'th degree polynomial modeling the random process $\eta_k(t)$. The statistics of the range residuals $r(t)$ may be developed from the covariance of the random clock errors. The second order statistics of the range residuals $r(t)$ to a polynomial model are obtained as

$$E[r(t)r^T(t)] = GE[R(t)R^T(t)]G^T \tag{42}$$

where

$$G = [I - A(A^TA)^{-1}A^T] \tag{43}$$

and A is the least squares design matrix for the polynomial model selected. The $E[R(t)R^T(t)]$ is the covariance matrix of the random clock error being modeled. This covariance is given by equations (32) and (33).

For integrated Doppler observations the statistics of the residuals to a given degree polynomial model are similarly obtained from equations (42) and (43), using the covariance matrix for integrated Doppler random error due to each system clock, equations (37) and (38). The equation may be written as

$$E[\Delta r(t)\Delta r^T(t)] = HE[\Delta R(t)\Delta R^T(t)]H^T \tag{44}$$

574

where the matrix H is similar to the matrix G of equation (43) with changes due to the choice of the model adopted for clock-induced random Doppler errors

$$H = [I - A'(A'A')^{-1}A']. \tag{45}$$

After the selection of the polynomial model, equation (40) has the form

$$\Delta\eta(t_\ell) = P_{is}(t_\ell) + P_{jk}(t_\ell) + \Delta r_s(t_\ell) + \Delta r_k(t_\ell) + \zeta_\ell. \tag{46}$$

If the statistics of these residuals were ignored in an estimation problem, then the resulting parameter covariance matrix would be optimistic. An increase in the degrees of the polynomial clock models would offset this optimism to some extent since the level of unmodeled error would be decreased. However, if a rigorous estimation is to be performed, then these residual statistics must be included in the weight matrix to account for the unmodeled error r(t) or Δr(t) in a statistical rather than parametric fashion. The estimation algorithm should then produce a valid parameter covariance matrix regardless of the order of the polynomial models used provided numerical problems are not encountered and the parameters are independent and well observed.

Finally, the theoretical standard errors for range residuals to a linear fit were determined using equation (42) for the rubidium and cesium clocks. The results are given in Figures 15 and 16. These figures graphically demonstrate that the statistics of the residuals to the clock modeling polynomial are not stationary. The variance of a residual depends on the order of the polynomial, the interval length and the location within the sample. However, the statistics of the residuals will be constant from interval to interval of the same length provided the sampling is performed equivalently and the same order polynomial is used.
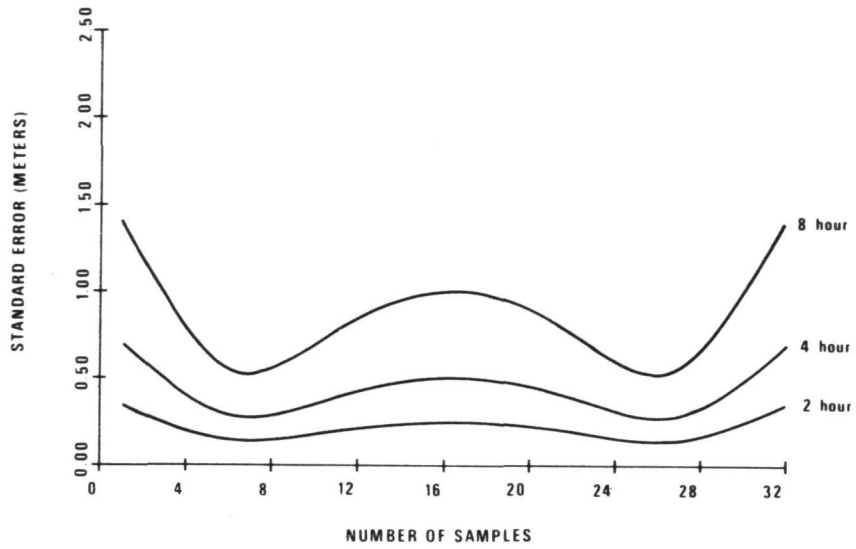
Fig. 15-Standard error of satellite rubidium
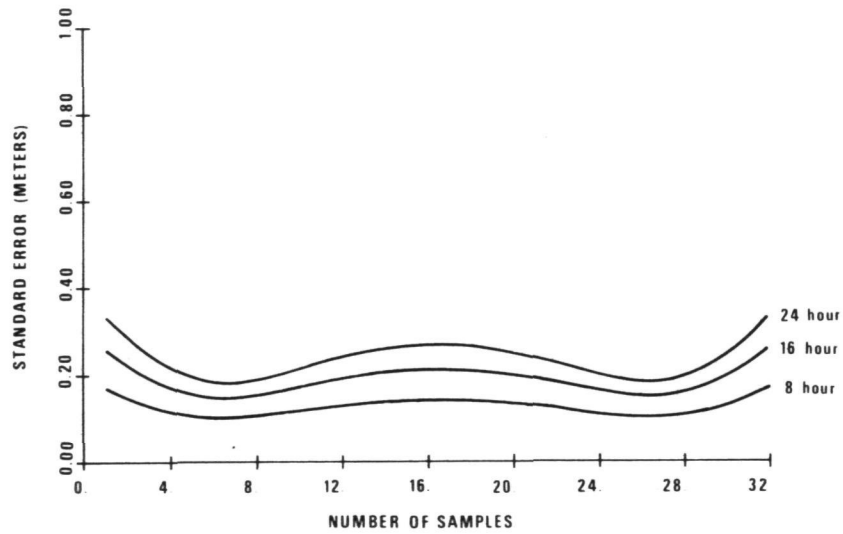clock residuals based on a linear fit

Fig. 16-Standard error of cesium clock
residuals based on a linear fit

REFERENCES

Allan, D. W., J. H. Shoaf, and D. Halford, 1974. "Statistics of Time and Frequency Data Analysis," Time and Frequency: Theory and Fundamentals, National Bureau of Standards Monograph 140, Blair (Editor).

Anderle, R. J., 1978. "Clock Performance as a Critical Parameter in Navigation Satellite Systems," Proceedings of the Tenth Annual Precise Time and Time Interval (PTTI) Applications and Planning Meeting, National Aeronautics and Space Administration Technical Memorandum 80250, Greenbelt, Maryland.

Barnes, J. A. and S. Jarvis, 1971. "Efficient Numerical and Analog Modeling of Flicker Noise Processes," National Bureau of Standards Technical Note 604, Boulder, Colorado.

Barnes, J. A., A. R. Chi, L. S. Cutler, D. J. Healey, D. B. Leeson, T. E. McGunigal, J. A. Mullen, Jr., W. L. Smith, R. L. Sydnor, R. F. C. Vessot, and G. M. R. Winkler, 1971. "Characterization of Frequency Stability," IEEE Transactions on Instrument and Measurements, Vol. 20, No. 2.

Bartholomew, C. A., 1978. "Satellite Frequency Standards," Navigation, Vol. 25, No. 2.

Blair, B. E. (Editor), 1974. Time and Frequency: Theory and Fundamentals, U. S. Department of Commerce/National Bureau of Standards Monograph 140, U. S. Government Printing Office, Washington, D.C.

Fell, P. J. and B. R. Hermann, 1979. "An Empirical Evaluation of the Effect of Oscillator Errors on Dynamic Point Positioning Based on the NAVSTAR GPS System," Proceedings of the Second International Geodetic Symposium on Satellite Doppler Positioning, Applied Research Laboratories, The University of Texas at Austin.

Fell, P. J., 1980. "Geodetic Positioning Using a Global Positioning System of Satellites," Department of Geodetic Science Report No. 299, The Ohio State University, Columbus.

Gelb, A., (Editor), 1974. Applied Optimal Estimation, MIT Press, Cambridge, Massachusetts.

Hellwig, H. W., 1975. "Atomic Frequency Standards: A Survey," Proceedings of the IEEE, Vol. 63, No. 2.

Hellwig, H. W., 1977. "Frequency Standards and Clocks: A Tutorial
    Introduction," National Bureau of Standards Technical Note 616,
    U. S. Government Printing Office, Washington, D.C.

Meditch, J. S., 1975. "Clock Error Models for Simulation and Estima-
    tion," The Aerospace Corporation, Report No. TOR-0076 (6474-01)-2,
    El Segundo, California.

QUESTIONS AND ANSWERS

DR. KARTASCHOFF:

I have just one question that you have been remodeling the flicker noise level with these five processes, and I was asking myself now when I hear it what do you think about if one just could use directly the time interval error estimation, as I had shown just before, also for estimating the range error?

Furthermore, one could try to estimate the uncertainty of that estimation by using the uncertainty of the Allan variance using the theory of Audoin-Lesage that limited the sample that we always, for a given time, τ, on the flicker level, and we always have an uncertainty that is given as the number of samples. For the last point you measured, you have only two samples; so you have 2000 percent error as the uncertainty.

I think it would be an interesting exercise to repeat the calculation using these estimations and using your process. Very probably both will give very similar results and both can be used. That would be interesting, I think.

MR. FELL:

I think you are right. This is just one way that you could do this approximate method, those Allan variances. They are specified for a clock and are only an approximation of actual performance, but for a long time people have ignored this type of residual error which is left in the estimation problem. And I think that because we are now trying to get down to such small errors, namely baseline errors of less than 10 centimeters, that we are going to have to take a second look at our modeling and make sure that it is sufficient for the problems that we are addressing.

Otherwise the parameter of statistics which we get out of the estimation algorithm are going to be too optimistic.

DR. VICTOR REINHARDT, NASA/Goddard

You also, if you do your conversions to your range statistics, or range rate statistics, up front you will find that your range rate estimator is one of the weighted Allan variances, and you can just use the tables that are published from converting to the zero dead time Allan variance to the Allan variance with dead times to get your range statistics. That all combined with some factor like C or $\frac{C}{\sqrt{2}}$.

And you can do this not even with a hand calculator on the back of an envelope, do the same thing just by looking up the NBS publications on the various weighings for the various models since all of the frequency standards that we use breakup into well defined regimes we have, you know, a well defined parallel.